Shock Tube and Modeling Study of the H + O_2 = OH + O Reaction over a Wide Range of Composition, Pressure, and Temperature

Si-Ok Ryu and Soon Muk Hwang

Department of Chemical Engineering, The University of Toledo, Toledo, Ohio 43606

Martin Jay Rabinowitz*

Internal Fluid Mechanics Division, NASA Lewis Research Center, Cleveland, Ohio 44135

Received: April 17, 1995; In Final Form: June 30, 1995[⊗]

The rate coefficient of the reaction H + O_2 = OH + O (1) was determined using OH laser absorption spectroscopy behind reflected shock waves over the temperature range 1050−2500 K and the pressure range 0.7−4.0 atm. Eight mixtures and three stoichiometries were used. Two distinct and independent criteria were employed in the evaluation of k_1. Our recommended expression for k_1 is $k_1 = 7.13 \times 10^{13} \exp(-6957\ K/T)$ cm^3 mol^{-1} s^{-1} with a statistical uncertainty of 6%. A critical review of recent evaluations of k_1 yields a consensus expression given by $k_1 = 7.82 \times 10^{13} \exp(-7105\ K/T)$ cm^3 mol^{-1} s^{-1} over the temperature range 960−5300 K. We do not support a non-Arrhenius rate coefficient expression, nor do we find evidence of composition dependence upon the determination of k_1.

Introduction

The reaction between hydrogen atom and oxygen molecule,

$$H + O_2 \rightarrow OH + O \quad (\Delta_r H^\circ_{298} = 70.2\ \text{kJ mol}^{-1}) \quad (1)$$

is the main chain branching reaction in the oxidation of hydrogen- and hydrocarbon-based fuels. About 80% of the oxygen in a typical atmospheric pressure hydrocarbon flame is consumed by this reaction.[1] That this reaction is rate controlling follows from its increase in both chain carriers and free valences and from its high activation energy (itself following from the high endothermicity). Thus, ignition delays and flame speeds, important and easily measurable combustion characteristics, are invariably found to be sensitive to the rate coefficient of this reaction.

The central role of reaction 1 in combustion chemistry has made it the object of intense scrutiny. In 1972, Baulch et al.[2] (BDHL) reviewed the available data and recommended the rate coefficient expression $k_1 = 2.2 \times 10^{14} \exp(-8450\ K/T)$ cm^3 mol^{-1} s^{-1}. They argued that the activation energy should not be less than the endothermicity based upon the bimolecular nature of the reaction and their expectation of a nonnegative activation energy of the reverse reaction (which was subsequently found to be negative).[3,4] In 1973, Schott[5] measured the exponential growth rate of CO_2 chemiluminescence in shock-heated $H_2/CO/O_2/Ar$ mixtures and reported a rate coefficient expression with a temperature-dependent preexponential factor, $k_1 = 1.22 \times 10^{17} T^{-0.907} \exp(-8369\ K/T)$ cm^3 mol^{-1} s^{-1}. For over a decade these two expressions formed the upper, BDHL, and lower, Schott, accepted limits for k_1, differing by a factor of 1.7 at 2000 K. In 1984, Warnatz[1] reviewed the available data and recommended Schott's expression. In 1985, Frank and Just[6] measured O and H atom concentration profiles in shock-heated $H_2/O_2/N_2O/Ar$ mixtures and reported the rate coefficient expression $k_1 = 2.44 \times 10^{14} \exp(-8697\ K/T)$ cm^3 mol^{-1} s^{-1}, which agreed well with the recommended value of BDHL; no temperature dependence of the preexponential factor was found. The position of experiment and review had been reversed with the experimental value now being a factor of 1.7 higher at 2000 K. This prompted a flurry of experimental and theoretical investigations of the title reaction using more advanced diagnostics and techniques.

Even though numerous experimental studies have been performed, disagreement still exists among the reported values of k_1. Schott[7] has suggested that this may be due not to differences in experimental techniques and data reduction methodologies but rather to differences in the reactant partial pressures used in the various studies, i.e., a composition effect. In this study we performed a series of experiments over a wide range of composition and pressure to explore the effect, if any, of reactant partial pressure upon the determination of k_1.

Experimental Section

Shock Tube System. The experimental setup is shown in Figure 1. Experiments were performed in a rolled square stainless steel shock tube 63.5 mm in cross section. Shocks were initiated by bursting an aluminum diaphragm with a cross-shaped knife-edge plunger. The test section was routinely pumped between experiments to 3×10^{-6} Torr using a Varian Turbo-V60 turbopump. A combined leak and outgassing rate of 5×10^{-6} Torr min^{-1} was measured. To further alleviate contamination, neither the driven nor driver sections was rough pumped below 500 mTorr. The gas handling system was constructed using Varian high-vacuum valves and fittings. Test gas pressures were measured using a Druck Model DPI-260 pressure transducer.

Two 25.4 mm diameter S1-UVA quartz windows, centered 12.7 mm from the end plate, were flush mounted with the shock tube inner walls. Shock passage was detected using four 113A21 PCB Piezotronics pressure transducers flush mounted with the shock tube inner wall, one of which was mounted at the axial position of the window center line. Shock velocities between each transducer pair were measured and fitted to a second-order polynomial in distance that was then used to obtain the extrapolated shock velocity at the end plate. Shock properties were computed using this velocity and standard methods[8] assuming full vibrational relaxation and no chemical reaction at the shock front. NASA thermochemical data[9] were

[⊗] Abstract published in *Advance ACS Abstracts,* August 15, 1995.

0022-3654/95/2099-13984$09.00/0

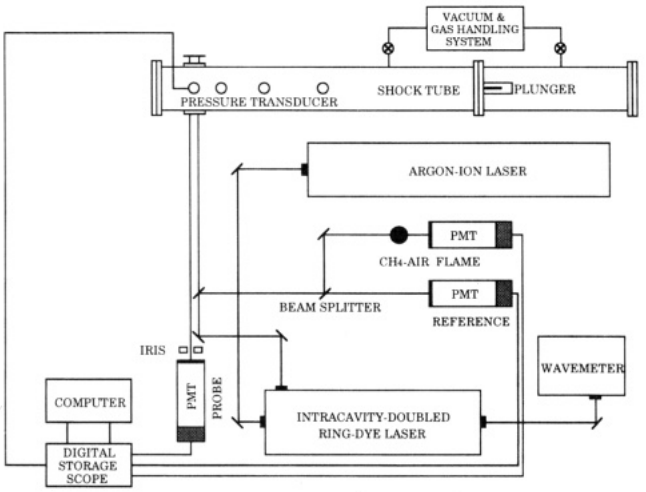

Figure 1. Schematic diagram of the experimental apparatus. The probe laser beam path is offset for clarity of presentation.

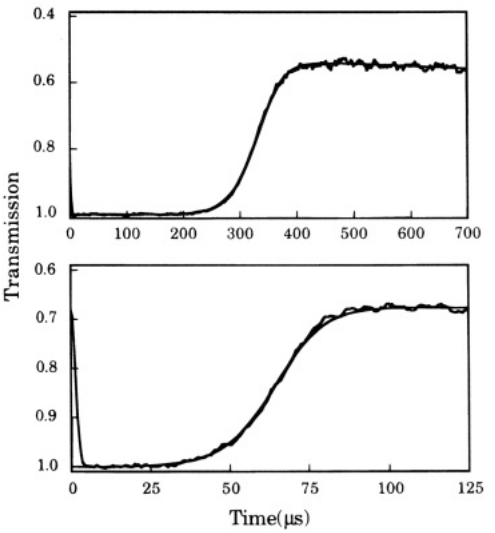

Figure 2. Typical experimental records. (a, top) 2.0% H_2, 0.5% O_2, 97.5% Ar, T_5 = 1556 K, and P_5 = 0.75 atm; (b, bottom) 2.0% H_2, 0.2% O_2, 97.8% Ar, T_5 = 2163 K, and P_5 = 1.99 atm. Spikes at time zero are schlieren signals due to reflected shock front passage. Smooth lines are computed OH absorption profiles using the Table 2 mechanism and the OH absorption coefficients determined from A_{max}.

used throughout the calculations. Computed shock properties were corrected for effects due to the interaction between the reflected shock front and the boundary layer following the adiabatic equation of state method described by Michael and Sutherland.[10] The postshock pressure, needed for the boundary layer correction, was measured using the pressure transducer centered above the windows. The initial test gas pressure was added to this pressure.

The temporal profile of OH concentration was monitored using the $P_1(5)$ line of the (0,0) band of the $A^2\Sigma^+ \leftarrow X^2\Pi$ transition at 310.032 nm (air). A Coherent CR-699-21 ring-dye laser running Kiton Red 620 dye was pumped by a Coherent Innova 200 argon ion laser. Dye solution temperature was maintained at 278 K to give optimum laser performance. Intracavity doubling via an angle-tuned $LiIO_3$ crystal produced a single-mode 5 mW UV beam with a 2 mm beam diameter. Center wavelength of the OH absorption line was determined by passing part of the UV beam through a burner-stabilized CH_4/air flame. The lasers, optical components, and the detection system described below were mounted on a pneumatically stabilized Newport MST series optical table.

Optical Detection System. A double-beam scheme was employed for signal detection. The UV beam was split into two beams. The first beam was directed through the shock tube at the center of the windows. If the expected absorbance for an experiment was small, the beam was reflected back through the shock tube at the same streamwise distance but vertically displaced from the incoming beam and onto the detector, i.e., double pass. For experiments with larger expected absorbance, the beam was returned to the detector after being steered around the shock tube, i.e., single pass. An iris was set in front of the detector both to limit the spurious signal due to hot gas emission from within the shock tube and to help establish "time zero", taken as the center of the schlieren signal caused by shock passage. The second beam was split again, and one part was directed to a reference detector and the other directed through a CH_4/air flame and onto a third detector. All three detectors were THORN EMI Model 9224QB photomultiplier tubes (PMT) using a five-dynode configuration to ensure optimum linearity. High-speed buffer/amplifiers were used to isolate the anodes. An overall electronic time constant of 0.2 μs was determined for the PMT/electronics/cable system. Background light reduction was achieved by mounting a narrow-band interference filter in front of each PMT. The reference, probe, difference (probe dc − reference ac), and the last pressure transducer signals were recorded on a four-channel Nicolet 4094C digital oscilloscope with Nicolet 4570 plug-in units. The pressure signal served as the trigger source for the oscilloscope. Reaction progress was followed using the difference signal. Further details of the experimental apparatus are given in ref 11.

Test Gas Mixtures. The test gas mixtures were prepared manometrically and allowed to stand for 48 h before use. The maximum uncertainty of the reactant concentration was 0.5% or less for each component. Gases were used as delivered with no further purification. Stated purities of the gases were as follows: H_2, 99.9995% (Linde Research Grade, THC as CH_4 <0.3 ppm); O_2, 99.6% (Linde Zero Grade, THC as CH_4 <0.3 ppm); Ar, 99.996% (Linde Zero Grade, THC as CH_4 <0.3 ppm). These purity levels were confirmed by gas chromatographic analysis with flame ionization detection.

Results

Typical transmission profiles at different experimental conditions are shown in Figure 2. After an induction period light absorption increases rapidly due to the essentially exponential growth of OH concentration caused by chain branching and propagation reactions. All experiments show rapid achievement of an OH superequilibrium concentration followed by a slow relaxation to equilibrium at long times.

Data reduction was accomplished using a small set of relevant information derived from the absorption traces, namely, A_{max} = $(1 - I/I_0)_{max}$, $NS_{max} = -d((I/I_0)/dt)_{max}/A_{max}$, and one characteristic time, t_{50}, the time at which the absorbed light intensity has reached 50% of A_{max}. These three observables were chosen based upon sensitivity analysis using a trial H_2/O_2 reaction mechanism. It has been shown previously[12,13] that a small number of appropriately chosen observables can embody the full information content of an experiment.

Experimental conditions, measured observables, and determined k_1 values are given in Table 1. Eight rich mixtures of equivalence ratios of 2, 5, and 10 were used. Mixture compositions were selected such that maximum absorption was less than 0.55 for all conditions. Reflected shock temperatures and pressures ranged from 1050 to 2500 K and from 0.7 to 4.0 atm, respectively. Temperatures obtained using the boundary layer correction were always higher than the ideal shock temperatures, on average by 1.4%. A clear dependence of the

TABLE 1: Experimental Conditions and Results[a]

T_5	P_5	A_{max}	NS_{max}	t_{50}	$k_1{}^b/10^{12}$	T_5	P_5	A_{max}	NS_{max}	t_{50}	$k_1{}^b/10^{12}$
					4.0% H_2, 1.0% O_2, 95.0% Ar ($\phi = 2$)						
1052	2.289	0.334	15 706	618	0.092	1102	0.960	0.344	7 252	836	0.124
1074	0.964	0.303	7 293	1005	0.104	1115	2.248	0.492	18 471	393	0.130
1086	0.940	0.294	6 642	985	0.112						
					2.0% H_2, 0.5% O_2, 97.5% Ar ($\phi = 2$)						
1155	0.957	0.215	4 646	1274	0.172	1570	0.737	0.267	12 205	316	0.933
1164	0.892	0.220	4 600	1283	0.179	1577	0.962	0.554	14 144	261	0.853
1170	0.950	0.232	4 887	1183	0.186	1578	0.788	0.463	11 241	308	0.829
1174	0.945	0.237	4 632	1153	0.181	1581	0.761	0.352	11 931	279	0.870
1228	0.734	0.227	4 656	1153	0.242	1596	0.852	0.503	12 898	269	0.894
1234	0.945	0.294	6 142	819	0.257	1627	0.738	0.315	13 234	250	1.05
1246	0.877	0.307	5 908	803	0.271	1649	0.733	0.488	12 854	272	1.07
1248	0.756	0.257	5 392	943	0.281	1652	0.769	0.328	13 076	242	1.06
1264	0.773	0.271	5 763	911	0.293	1667	0.744	0.499	13 801	253	1.15
1274	0.781	0.302	5 874	814	0.312	1708	0.771	0.517	14 116	228	1.20
1285	0.794	0.294	6 323	794	0.325	1715	0.797	0.361	15 958	220	1.32
1313	0.936	0.326	7 150	616	0.338	1726	0.784	0.364	14 513	214	1.24
1323	0.800	0.310	7 354	696	0.386	1747	0.795	0.344	16 398	204	1.41
1352	0.766	0.351	7 866	620	0.433	1760	1.034	0.480	20 408	150	1.39
1357	0.771	0.356	7 162	612	0.420	1809	0.846	0.409	18 716	161	1.55
1358	0.772	0.353	7 886	633	0.439	1915	0.876	0.407	23 206	129	2.08
1359	0.774	0.354	7 183	611	0.419	1924	0.735	0.393	17 442	146	1.88
1387	0.778	0.368	7 777	537	0.474	1998	1.018	0.484	25 570	99	2.03
1472	0.859	0.437	10 011	384	0.601	2017	0.757	0.429	21 440	128	2.40
1516	0.699	0.226	9 331	453	0.707	2030	0.854	0.430	23 325	113	2.27
1556	0.751	0.460	10 965	329	0.820	2099	0.772	0.450	22 173	108	2.48
1558	0.733	0.445	10 885	343	0.837	2136	0.851	0.487	24 733	92	2.78
					0.4% H_2, 0.1% O_2, 99.5% Ar ($\phi = 2$)						
1525	2.005	0.210	5 742	703	0.734	2068	1.819	0.390	9 848	236	2.32
1639	2.049	0.270	6 744	550	1.00	2082	1.857	0.375	10 229	224	2.35
1692	2.029	0.284	7 447	432	1.17	2132	2.094	0.439	13 291	185	2.83
1934	1.922	0.341	10 058	293	2.07	2256	2.050	0.439	13 567	163	3.10
2044	2.146	0.438	12 744	199	2.52	2409	2.095	0.453	15 403	127	3.67
					0.2% H_2, 0.05% O_2, 99.75% Ar ($\phi = 2$)						
1527	3.770	0.156	5 948	647	0.753	1888	3.880	0.242	9 066	270	1.77
1593	3.704	0.143	6 720	534	0.912	1977	4.050	0.271	10 560	203	2.09
1658	3.654	0.168	6 928	476	1.09	1999	3.697	0.224	9 383	237	2.08
1716	3.792	0.217	7 281	397	1.24	2001	4.088	0.276	11 847	203	2.35
1725	3.905	0.233	7 652	360	1.27	2092	3.681	0.257	11 431	193	2.66
1763	3.843	0.195	8 179	356	1.41	2211	3.715	0.270	12 714	158	3.14
					5.0% H_2, 0.5% O_2, 94.5% Ar ($\phi = 5$)						
1243	0.798	0.084	6 857	863	0.259	1637	0.760	0.171	18 093	216	1.03
1246	0.795	0.086	7 325	822	0.272	1675	0.749	0.160	18 556	200	1.13
1251	0.792	0.091	7 274	784	0.276	1684	0.758	0.199	19 331	191	1.17
1252	0.800	0.084	7 083	807	0.267	1706	0.739	0.160	18 381	190	1.18
1254	0.813	0.089	7 595	799	0.282	1743	0.749	0.231	19 012	168	1.26
1301	0.754	0.101	8 099	643	0.337	1754	0.702	0.230	17 430	177	1.26
1315	0.766	0.112	8 580	581	0.359	1805	0.756	0.264	20 371	140	1.43
1330	0.784	0.108	9 342	578	0.387	1897	0.761	0.293	23 894	121	1.80
1333	0.793	0.108	9 490	578	0.391	1939	0.728	0.260	24 669	118	2.02
1336	0.797	0.110	9 645	574	0.368	2014	0.721	0.265	23 294	105	2.11
1336	0.794	0.107	9 009	559	0.392	2015	0.746	0.290	25 968	102	2.25
1337	0.796	0.114	9 631	561	0.395	2038	0.849	0.311	29 993	86	2.34
1516	0.768	0.168	14 101	274	0.722	2041	0.732	0.298	23 761	98	2.18
1538	0.794	0.152	14 815	280	0.755	2125	0.721	0.324	27 141	88	2.69
1543	0.744	0.164	13 298	269	0.725	2151	0.724	0.337	26 430	84	2.69
1546	0.799	0.152	15 348	269	0.777	2188	0.775	0.343	28 553	74	2.78
1549	0.794	0.178	16 252	257	0.822	2376	0.756	0.383	33 464	58	3.69
1565	0.810	0.198	16 257	235	0.833	2414	0.725	0.366	32 218	57	3.84
1620	0.759	0.196	15 790	220	0.910						
					2.0% H_2, 0.2% O_2, 97.8% Ar ($\phi = 5$)						
1509	1.629	0.098	12 846	338	0.736	2029	1.613	0.219	23 397	106	2.36
1522	1.754	0.107	13 364	313	0.760	2049	1.578	0.197	24 015	103	2.50
1531	1.673	0.108	14 009	321	0.802	2094	1.816	0.271	28 007	81	2.65
1578	1.682	0.126	13 023	264	0.808	2134	1.783	0.294	28 023	78	2.80
1667	1.725	0.154	16 084	209	1.06	2163	1.994	0.323	32 160	64	2.95
1746	1.744	0.170	20 747	165	1.44	2165	1.981	0.294	31 462	67	2.91
1819	1.757	0.195	22 707	144	1.69	2184	1.780	0.289	29 065	71	3.02
1850	1.759	0.184	20 516	136	1.60	2282	1.849	0.265	31 781	59	3.41
1884	1.893	0.223	24 345	116	1.81	2293	1.852	0.303	31 250	58	3.38
1948	1.834	0.215	24 065	106	1.98	2345	1.915	0.358	34 435	52	3.70
1989	1.579	0.201	21 756	113	2.16	2379	2.024	0.372	36 669	47	3.81
1997	1.838	0.229	24 397	97	2.11	2501	2.013	0.356	40 415	40	4.46
2026	1.786	0.244	25 774	95	2.34						

TABLE 1 (Continued)

T_5	P_5	A_{max}	NS_{max}	t_{50}	$k_1{}^b/10^{12}$	T_5	P_5	A_{max}	NS_{max}	t_{50}	$k_1{}^b/10^{12}$
1.0% H_2, 0.1% O_2, 98.9% Ar (ϕ = 5)											
1521	3.263	0.090	11 966	328	0.724	1895	3.285	0.179	19 508	130	1.72
1533	3.303	0.075	13 013	323	0.760	1913	3.378	0.183	20 306	118	1.76
1557	3.382	0.088	14 556	280	0.850	1945	3.117	0.195	19 707	126	1.91
1579	3.054	0.104	13 067	286	0.888	1976	3.280	0.189	20 783	111	1.97
1583	3.510	0.106	13 726	246	0.818	2057	3.329	0.195	25 794	93	2.55
1609	3.387	0.091	13 219	241	0.833	2104	3.439	0.253	26 296	82	2.65
1611	3.720	0.109	15 339	224	0.881	2107	3.403	0.251	24 083	84	2.49
1647	3.342	0.100	15 969	231	1.05	2142	3.444	0.208	26 735	77	2.78
1664	3.868	0.123	18 219	185	1.07	2155	3.383	0.223	25 695	77	2.75
1700	3.203	0.117	17 128	201	1.25	2213	3.370	0.224	28 098	67	3.13
1714	3.237	0.120	16 308	197	1.19	2305	3.442	0.255	31 545	59	3.65
1792	3.275	0.144	20 541	165	1.59	2355	3.478	0.229	31 423	53	3.73
1809	3.331	0.148	19 533	153	1.53	2379	3.313	0.249	31 052	56	3.91
1841	3.811	0.157	20 503	122	1.46	2413	3.384	0.262	32 645	49	4.10
1846	3.364	0.150	20 213	138	1.61						
10.0% H_2, 0.5% O_2, 89.5% Ar (ϕ = 10)											
1514	0.722	0.075	15 079	288	0.746	1801	0.784	0.132	25 310	127	1.52
1569	0.804	0.096	17 854	229	0.845	1869	0.851	0.169	27 958	104	1.67
1575	0.809	0.093	19 172	217	0.904	1883	0.850	0.148	30 587	102	1.82
1579	0.718	0.091	16 901	226	0.900	2042	0.836	0.143	34 097	74	2.41
1616	0.796	0.086	20 406	193	1.01	2081	0.861	0.157	36 968	68	2.63
1698	0.812	0.115	24 913	155	1.30	2407	0.897	0.206	47 300	39	4.16
1715	0.827	0.117	25 299	152	1.32	2481	0.902	0.211	47 061	36	4.31
1782	0.978	0.136	29 323	104	1.39	2494	0.856	0.215	45 520	37	4.42

[a] Units are K for T_5, atm for P_5, s^{-1} for normalized maximum slope, μs for t_{50}, and cm^3 mol^{-1} s^{-1} for k_1. [b] $k_1(NS_{max})$.

correction upon the ideal shock temperature or the initial pressure was not observed. Post shock reactant densities ranged from 4×10^{-8} to 7×10^{-7} mol cm^{-3} for H_2 and 1×10^{-8} to 3×10^{-7} mol cm^{-3} for O_2. The upper bound for the experimental temperature range was set by the appearance of absorption in a series of shocks in a 2% O_2/98% Ar mixture, presumably from hydrocarbon contamination. At temperatures above 2700 K a small but noticeable absorption was observed at long times. We speculate that H atom producing contaminants swept off the shock tube walls or in the test gas may be responsible. The lower temperature bound of 1050 K was set by the loss of absorption signal due to the diminishing amount of OH generated at lower temperatures.

Computer simulations were performed using the detailed reaction mechanism of Yuan et al.,[14] with the following modifications: the rate coefficient for OH + H_2 = H_2O + H(3) was taken from the review of Oldenborg et al.,[15] the rate coefficient for O + H_2O = OH + OH (4) was taken from the review of Michael,[16] and the reaction H + O + M = OH + M (7) was added with the rate coefficient and third body efficiencies from Masten et al.[17] The reaction mechanism and rate coefficient expressions are given in Table 2. Reverse reaction rate coefficients were calculated from the principle of detailed balancing. NASA thermochemical data[9] were used in all calculations. The LSODE integrator[18] was used to solve the set of stiff differential equations describing chemical reaction under the assumed constant-density conditions for reflected shocks.[8]

Local logarithmic response sensitivities[19] computed for the Figure 2 experimental conditions are shown in Figure 3. Overall, NS_{max} and t_{50} are sensitive only to reaction 1. Therefore, k_1 could be determined by matching NS_{max} or t_{50}; however, the effect of possible contaminants must be considered. This effect can be readily simulated by assuming that H atoms are present in the initial mixture. At high temperatures H atoms are generated by fast initiation reactions of the H_2/O_2 system so that the addition of contaminants is found to have little effect; e.g., addition of 50 ppb H atoms to a 2% H_2/0.2% O_2/97.8% Ar mixture at 2163 K changed t_{50} from 65.4 to 65.1 μs. At low temperatures H atom contamination has a profound effect upon t_{50}; e.g., addition of 5 ppb H atoms to a 2% H_2/0.5% O_2/97.5% Ar mixture at 1234 K changed t_{50} from 824 to 693 μs. This reduction in t_{50} is equivalent to a 23% increase in k_1. NS_{max} is unaffected by H atom addition for either case.

TABLE 2: Reaction Mechanism[a]

reaction	A^b	n	θ	ref
1. H + O_2 = OH + O	7.13 (+13)	0.0	6957	this study
2. O + H_2 = OH + H	1.87 (+14)	0.0	6854	38
3. OH + H_2 = H_2O + H	2.14 (+08)	1.52	1736	15
4. O + H_2O = OH + OH	4.51 (+04)	2.70	7323	16
5. O + O + M = O_2 + M (Ar = 1.0, H_2 = 2.9, O_2 = 1.2, H_2O = 18.5)	1.00 (+17)	−1.0	0	12
6. H + H + M = H_2 + M (Ar = 1.0, H_2 = 4.0, H_2O = 12.0, H = 26.0)	6.40 (+17)	−1.0	0	12
7. H + O + M = OH + M (Ar = 1.0, H_2O = 5.0)	6.17 (+16)	−0.6	0	17
8. H + OH + M = H_2O + M (Ar = 1.0, H_2 = 2.5, H_2O = 16.25)	8.40 (+21)	−2.0	0	12
9. H + O_2 + M = HO_2 + M (Ar = 1.0, H_2 = 3.33, O_2 = 1.33, H_2O = 21.3)	7.00 (+17)	−0.8	0	12
10. HO_2 + H = OH + OH	2.20 (+14)	0.0	710	39
11. HO_2 + H = H_2 + O_2	2.50 (+13)	0.0	350	1
12. HO_2 + H = H_2O + O	5.00 (+12)	0.0	710	39
13. HO_2 + O = O_2 + OH	2.00 (+13)	0.0	0	1
14. HO_2 + OH = H_2O + O_2	2.00 (+13)	0.0	0	1
15. HO_2 + HO_2 = H_2O_2 + O_2	1.06 (+11)	0.0	−855	40
16. H_2O_2 + M = OH + OH + M (Ar = 0.67, O_2 = 0.78, H_2O = 6.0)	1.20 (+17)	0.0	22900	12
17. H_2O_2 + H = HO_2 + H_2	1.70 (+12)	0.0	1900	1
18. H_2O_2 + H = H_2O + OH	1.00 (+13)	0.0	1805	1
19. H_2O_2 + O = HO_2 + OH	2.80 (+13)	0.0	3225	40
20. H_2O_2 + OH = H_2O + HO_2	7.00 (+12)	0.0	720	1

[a] Rate coefficients are in the form $k = AT^n \exp(-\theta/T)$. Units are K, cm^3, mol, and s. [b] Numbers in parentheses are powers of 10.

Based upon the sensitivity and contaminant effect studies, k_1 and ϵ(OH) were the parameters chosen for simultaneous optimization using NS_{max} and A_{max} as the target criteria. It should be noted that t_{50}, an integral measure of reaction progress, is affected by the details of initiation, whereas NS_{max}, a differential measure of growth, is determined at a point in reaction progress where memory of the initiation process is lost.

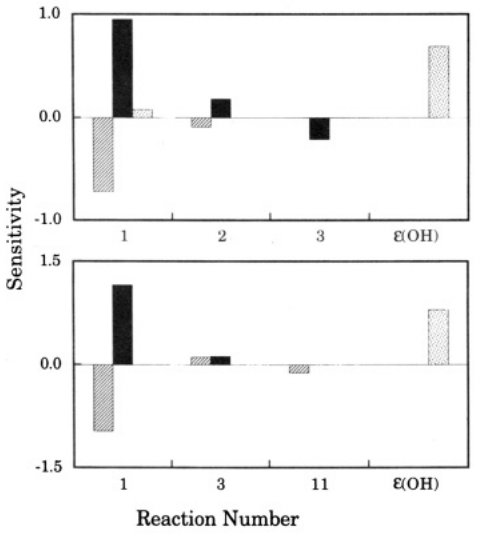

Figure 3. Sensitivity spectra for the experimental conditions in Figure 2a,b. Sensitivities are for 30% increase to Table 2 values and absorption coefficients. Reaction numbers are listed in Table 2. ■, for NS_{max} sensitivity; ⊡, for A_{max} sensitivity; hashed □, for t_{50} sensitivity.

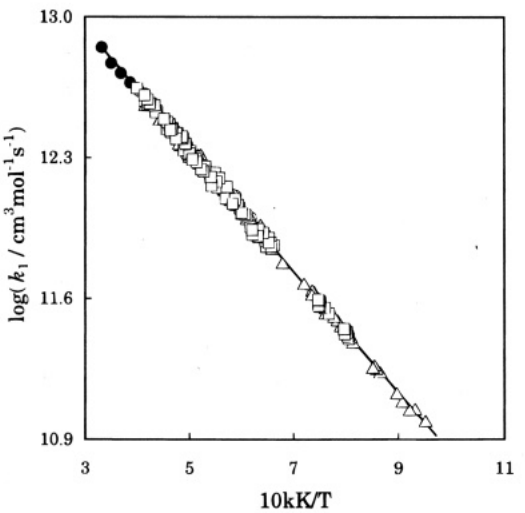

Figure 4. Arrhenius plot of the experimental data for $k_1(NS_{max})$. The solid line is the least-squares fit to the data; $k_1(NS_{max}) = 7.13 \times 10^{13}$ exp(−6957 K/T) cm^3 mol^{-1} s^{-1} (1050 K ≤ T ≤ 2500 K). Symbols are △ for $\phi = 2$ mixtures, □ for $\phi = 5$ mixtures, ○ for $\phi = 10$ mixtures, and ● for $\phi = 15$ mixtures (15.0% H_2, 0.5% O_2, 84.5% Ar). The data for $\phi = 15$ mixtures were not included in the least-squares fit for $k_1(NS_{max})$.

The data obtained above 2500 K were not included in the analysis due to possible contamination effects (see above). However, as can be seen in Figure 4, these points lie on the extrapolated line. A least-squares fit to the data is given by

$$k_1(NS_{max}) = (7.13 \pm 0.31) \times 10^{13} \exp(-6957 \pm 30\ \text{K}/T)\ \ \text{cm}^3\ \text{mol}^{-1}\ \text{s}^{-1}$$

with a 4% standard deviation, over the temperature range 1050−2500 K.

As was shown previously, k_1 and ϵ(OH) can be determined using t_{50} and A_{max} as the optimization criteria if possible contamination effects are ignored. Results of this analysis are shown in Figure 5 where the solid line represents the least-squares fit to the data given by:

$$k_1(t_{50}) = (7.19 \pm 0.41) \times 10^{13} \exp(-7015 \pm 40\ \text{K}/T)\ \ \text{cm}^3\ \text{mol}^{-1}\ \text{s}^{-1}$$

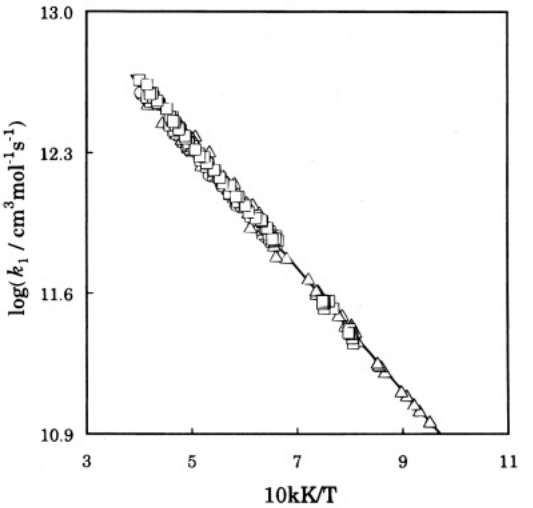

Figure 5. Arrhenius plot of the experimental data of $k_1(t_{50})$. The solid line is the least-squares fit to the data; $k_1(t_{50}) = 7.19 \times 10^{13}$ exp(−7015 K/T) cm^3 mol^{-1} s^{-1}. Symbols as in Figure 4.

with a 6% standard deviation, over the same temperature range. The choice of optimization criteria results in two slightly different Arrhenius expressions that diverge with decreasing temperature for a maximum difference of 5% at the low-temperature extreme. If there were contamination effects, we would have expected that the expressions should have been quite different due to the dramatic effect of impurities upon t_{50}. The agreement of these two expressions implies that our experimental results were not significantly influenced by the presence of impurities.

A standard propagation-of-error analysis[20] was performed for individual experimental determinations of k_1. Contributions to uncertainty were estimated using the measurement accuracy of the various transducers and oscilloscopes. Maximum uncertainties in the determination of $k_1(NS_{max})$ and $k_1(t_{50})$ were 6.0% and 7.5%, respectively. These values were then used as error limits instead of the smaller values derived from the scatter of the data about the fitted Arrhenius expressions. For typical conditions the percentage contribution to the uncertainty for individual $k_1(NS_{max})$ values are 54% from NS_{max}, 24% from P_5 in the temperature correction, 10% from incident shock velocity, and 10% and 2% from ΔX_{O_2} and ΔX_{H_2} of the initial mixture composition, respectively. A similar distribution of the uncertainty contributions was also obtained for $k_1(t_{50})$.

Shown in Figure 2 are computed profiles (smooth lines) obtained using the reaction mechanism in Table 2. As can be seen, the computed profiles reproduce the experiments quite well. Inspection of Figures 4 and 5 reveals that the k_1 values exhibit no dependence upon either composition or pressure over the ranges investigated in this study.

Discussion

The present determination of k_1 is compared to recent experimental and modeling studies in Table 3 and Figure 6. There is good agreement with the expressions of Shin and Michael[21] and Yang et al.[22]

The study of Pirraglia et al.[23] (PMSK), flash photolysis followed by pseudo-first-order decay of H atoms, has taken on an great importance because it contains the only data for k_1 below 1050 K. As a result, it has been used in most of the more recent studies either for comparison[14,17,21] or combined with other data to make Arrhenius[24] or non-Arrhenius[17] expressions. While the expressions determined by PMSK and in this study agree within 20% over the mutual temperature range, their

TABLE 3: Comparison of Rate Coefficient Expressions[a]

authors[b]	T range	A	n	θ	ref	notes
PMSK	962−1750	$(1.68 \pm 0.19) \times 10^{14}$	0.00	8119 ± 139	23	*c*
MHB	1450−3370	$(9.33 \pm 0.40) \times 10^{13}$	0.00	7448 ± 86	17	*d*
YWYFR	1050−2700	1.59×10^{17}	−0.927	8493	14	*e*
SM	1103−2055	$(6.93 \pm 0.96) \times 10^{13}$	0.00	6917 ± 193	21	*d*
DH	960−5300	$(9.76 \pm 0.72) \times 10^{13}$	0.00	7474 ± 122	24	*f*
YFMHB	1336−3370	8.30×10^{13}	0.00	7253	27	*g*
YGSF	1100−3550	$(7.60 \pm 0.70) \times 10^{13}$	0.00	7065 ± 140	22	*h*
RHR	1050−2500	$(7.13 \pm 0.31) \times 10^{13}$	0.00	6957 ± 30	this study	*i*

[a] Rate coefficients are in the form $k = AT^n \exp(-\theta/T)$. Units are K, cm^3, mol, and s. [b] Abbreviations explained in text. [c] 16% mean deviation. [d] 1σ deviation. [e] $\sigma_{\log k} = 0.05$. [f] Uncertainties in 95% confidence level; combined results with SM, MHB, PMSK data. [g] 9% 1σ deviation; optimization using YWYFR and MHB data. [h] 1σ deviation; combined results with SM data. [i] 6% deviation, $k_1(NS_{max})$.

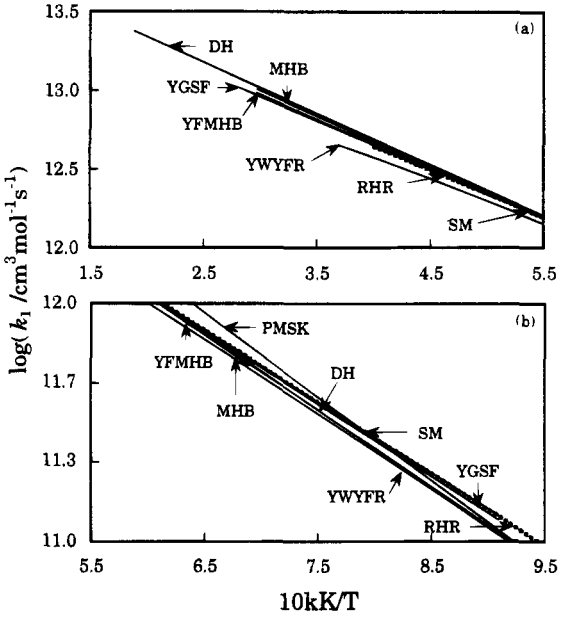

Figure 6. Comparison of the present results for k_1 to the previous experimental studies.

temperature dependences are very different. At 1050 K our expression is 22% higher, and at 1700 K our expression is 19% lower. A recent review[16] notes that there may have been bias in the data set at low temperatures (T < 1200 K) due to a systematic overestimation of HO_2 production. This may account for the high-temperature dependence observed by PMSK.

Masten et al.[17] (MHB) performed a dual beam laser absorption study of OH radical similar to ours. They obtained an expression that is 7.5% higher at 2500 K and 7.0% lower at 1450 K than the present study; however, our expression is contained within the MHB error limits (±10%). For the incident shock condition shown in Figure 3 of MHB our value of k_1 is 2% lower than their value, and as might be expected, our predicted profile is in excellent agreement with the MHB experimental profile. For the reflected shock condition shown in their Figure 5 our value of k_1 is 10% lower. Nonetheless, our predicted profile is again in good agreement with their experimental profile. Substitution of our k_1 expression into the MHB mechanism required a factor of 2.5 increase in the value of the initiation reaction, k_{11} ($HO_2 + H = H_2 + O_2$), to match the profile. This is an increase of only 40% above the value of k_{11} used in the present study. In their analysis MHB treated k_{11} as a profile shifting parameter, the shape of the profile being controlled by k_1.

Yuan et al.[14] (YWYFR) performed a single-beam laser absorption study of OH radical. Five active parameters, k_1, k_2, k_3, k_{11}, and $\Delta_f H°_{298}(HO_2)$, were simultaneously optimized using the solution mapping method.[25] Compared to the present results in the common temperature range, 1150−2500 K, the k_1 values of YWYFR are on average 14% lower, but the error limits are overlapped. These authors also reported that when using MHB's secondary reaction rate coefficients, k_2, k_3, and k_{11}, a slightly different expression resulted, $1.71 \times 10^{17} T^{-0.932} \exp(-8498\ K/T)$, which differs from their previous expression by 3% and shows the effect of the choice of secondary reaction rate coefficients upon the determination of k_1.

Shin and Michael[21] (SM) performed a laser photolysis study of H atom depletion under pseudo-first-order conditions. As shown in Figure 6, the k_1 values of SM and those of the present study are in agreement over the temperature range 1100−2055 K. Their k_1 values, derived from the measured slope of ln(absorbance)$_t$, are independent of impurity effects. SM corrected for boundary layer effects as was done in the present study.[10,26]

Du and Hessler[24] (DH) performed a flash absorption study of OH radical profiles in shock-heated $H_2/O_2/Kr$ test gas. They combined their results with the data of MHB, PMSK, and SM and obtained an expression that is 16% lower at 1050 K and 11% higher at 2500 K than the present results. In their evaluation DH introduced a profile shift parameter, x_c, that was needed to shift their calculated profiles to longer distances in order to match the experimental profiles. They associated x_c with the incubation time of H_2 dissociation, the main initiation channel at high temperature. However, we are able to model their Figure 3 experimental profile using the Table 2 mechanism without any profile shifting. This comparison is shown in Figure 7, where the solid line is our predicted absorption profile and the dotted lines are the upper and lower noise band of the DH profile. For this condition DH used a 0.783 mm shift of their calculated profile. Our prediction is well within the noise band, although approaching the high end at long distances, where the profile is controlled by H_2 decomposition. Indeed, at all times, the profile is more sensitive to the rate coefficient of H + H + M = H_2 + M (6) than to all other reactions, including reaction 1. This can be seen in Figure 7 where the upper filled boxes and the lower open boxes represent the extent of profile shift for ±20% variations in k_1 and k_6, respectively.

Recently, the data of YWYFR and MHB were subjected to a simultaneous optimization using two different model responses by Yu et al.[27] (YFMHB): the characteristic times, t_i, and the time difference, Δt, defined as $\Delta t = t_{75} - t_{25}$. The MHB data yielded nearly identical k_1 expressions for both model responses while those of YWYFR were noticeably different, with $k_1(t_i)$ having a nonzero temperature dependence of the preexponential factor and being 15% lower than $k_1(\Delta t)$ at 2150 K. There was reasonable agreement between the YWYFR $k_1(\Delta t)$ and both the MHB k_1 expressions (which were nearly identical). An explanation for the difference between the YWYFR $k_1(t_i)$ and $k_1(\Delta t)$ was proposed on the basis of the effect of vibrational nonequilibrium of O_2. The high-temperature YWYFR data were taken at short reaction times where this effect would be most pronounced. This is akin to the explanation given by DH for

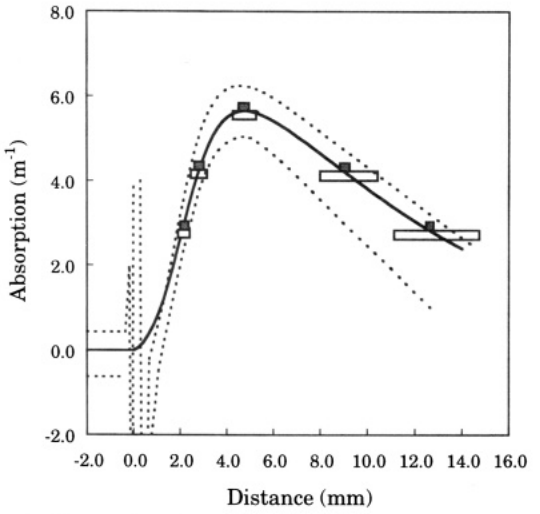

Figure 7. Comparison of our computed profile to the experimental profile of Du and Hessler's Figure 3 condition.[24] The solid line is the absorption profile computed using the Table 2 reaction mechanism with $x_c = 0$. The dotted lines are upper and lower noise band derived from the DH profile. The early part of the experimental signal is dominated by shock passage transients. Filled and open boxes represent the extent of profile changes for ±20% variation of k_1 (H + O_2 = OH + O) and k_6 (H + H + M = H_2 + M), respectively.

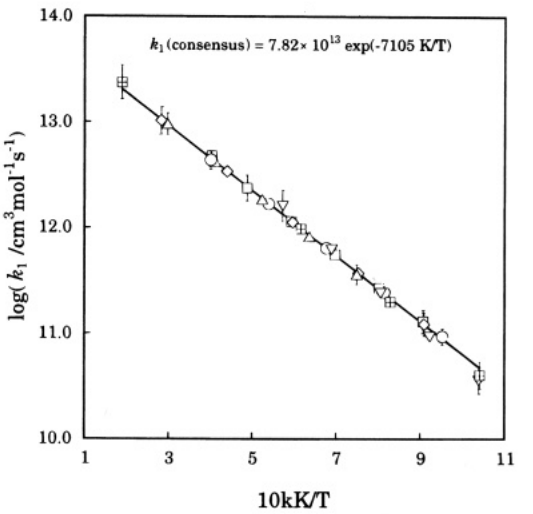

Figure 8. Consensus expression for k_1. Solid line is the consensus expression; $k_1(NS_{max})$ = 7.82 × 10^{13} exp(−7105 K/T) cm^3 mol^{-1} s^{-1} (960 K ≤ T ≤ 5300 K). Symbols: ▽, PMSK; crossed □, DH; □, SM; △, YFMHB; ◇, YGSF; ○, RHR. Uncertainty limits for the individual expressions are shown for the highest and lowest temperature points.

the profile shift parameter included in their study. YFMHB suggest an Arrhenius expression based upon the Δt response surface that is within our error bounds, being 3% higher at 2500 K and 7% lower at 1336 K than the present study.

The possible effect of O_2 vibrational relaxation on hydrogen combustion has important implications for the prediction of air-breathing hypersonic propulsion system performance. Such systems would be hydrogen fueled and have characteristic chemical reaction times much shorter than 100 μs. In order to quantify the effect of O_2 vibrational relaxation, a series of experiments were run using the YWYFR Series E composition in the pressure and temperature range where the effect should be most apparent, i.e., 2.4−3.0 atm and 1905−2380 K. Unlike the case of the YWYFR data, we did not see a difference between the k_1 value determined using either t_{50} or Δt as the modeling criterion. The experimental values of t_{50} and Δt are shorter than predicted using the Table 2 mechanism, on average by 2% (0.6 μs) and 5% (0.3 μs), respectively. While arbitrary time accuracy may be achieved in simulations, differences of this scale, although they are discernible, are not particularly meaningful. Nonetheless, the Table 2 mechanism does account for the t_{50}, Δt, and NS_{max} values for each experiment. At these conditions there is exquisite sensitivity to t_{50} as modeling criterion—a 0.1 μs change requires a 1% change in k_1, while sensitivity to Δt was smaller. The optimized k_1 values for these experiments differ on average by 4% (within our uncertainty limits) from our recommended expression. Individual experiments required adjustments between −3% and +8%. We are not required to invoke O_2 vibrational relaxation to explain our short reaction time data as both t_{50} and Δt are predicted equally well using our mechanism without additional constraints. Belles and Lauver[28] have previously shown that O_2 vibrational relaxation is not required to explain the induction delay lengthening at short times in H_2/O_2 mixtures as had been proposed by Schott and Kinsey.[29]

Yang et al.[22] (YGSF) performed a single-beam laser absorption study of OH radical. It was a reinvestigation that supplanted previous work on the title reaction.[30,31] An iterative optimization using eight time-difference responses (e.g., $t_{50} - t_{40}$) yielded a rate coefficient expression that is 5% lower at 1850 K and 5% higher at 2500 K than our expression. YGSF then combined their data with that of SM and obtained a new expression that is also within our error bounds, being 4% lower at 1100 K and 2% higher at 2500 K.

Both experimental and theoretical proposals have been made for the temperature dependence of the preexponential factor of k_1. Nonzero experimental values are reported by Schott (−0.907), YWYFR (−0.927), and MHB (−0.7, obtained from the combination of MHB and PMSK data). Miller's theoretical calculation gave −0.816[32,33] obtained using quasiclassical trajectory and quantum mechanical threshold methods on the potential energy surface of Melius and Blint.[34] He attributed the negative temperature dependence to the nonstatistical "recrossing" effects especially at high temperatures. PMSK, MHB (MHB data only), SM, DH, YFMHB, YGSF, and the present study do not find a temperature dependence for the preexponential factor. Recently, Varandas et al.[35] (VBP) calculated the thermal rate coefficient using various versions of quasiclassical trajectory method at 1000, 1750, 2000, 2500, and 3000 K. In the calculation, the fourth version of their double many-body expansion potential energy surface[36] for the ground state of HO_2 was utilized, which reproduces the most accurate estimates of the experimental dissociation energy, equilibrium geometry, and quadratic force constants. Their calculations showed no temperature dependence for the preexponential factor.

There exists reasonable agreement between the results of this study and most of the recent evaluations of k_1,[21−24,27,37] and so it is possible to achieve a consensus expression, shown in Figure 8, given by

$$k_1 = 7.82 \times 10^{13} \exp(-7105\ \mathrm{K}/T)\ \ \mathrm{cm^3\ mol^{-1}\ s^{-1}}$$

over the temperature range 960−5300 K, with an uncertainty of 6%. We developed this expression in the following fashion. The expressions of PMSK, SM, DH, YFMHB, YGSF, and the present study were converted to a series of "data points" evenly spaced in 1/T over their temperature ranges. A weighted least-squares fit was then obtained with the weighting factor taken as the inverse of the uncertainty limits for the Arrhenius expressions reported in the individual studies. The data of PMSK and SM were used to develop the DH expression, and the data of SM were used to develop the YGSF expression.

Accordingly, their weighting factors were reduced, PMSK by half and SM by two-thirds, to correct for their overrepresentation. An Arrhenius expression was assumed as there is neither an experimental nor, currently, a theoretical basis for curvature.

Conclusions

The rate coefficient of the reaction H + O_2 = OH + O (1) was determined using OH laser absorption spectroscopy behind reflected shock waves over the temperature range 1050−2500 K and the pressure range 0.7−4.0 atm. Eight different mixtures and three different stoichiometries were used. Two distinct and independent criteria were employed in the evaluation of k_1, namely, normalized maximum slope and the characteristic time, t_{50}. Our recommended expression for k_1, obtained using normalized maximum slope, is

$$k_1 = 7.13 \times 10^{13} \exp(-6957\ \mathrm{K}/T)\ \ \mathrm{cm^3\ mol^{-1}\ s^{-1}}$$

with an uncertainty of 6%. This expression agrees with that of SM and with the computational results of VBP. We neither support a curved rate coefficient expression nor find evidence of composition dependence upon the determination of k_1. Without confirmation of the PMSK results below 1050 K, there is neither an experimental nor, currently, a theoretical basis for curvature. Critical review of recent k_1 determinations yields the consensus expression

$$k_1 = 7.82 \times 10^{13} \exp(-7105\ \mathrm{K}/T)\ \ \mathrm{cm^3\ mol^{-1}\ s^{-1}}$$

over the temperature range 960−5300 K.

Acknowledgment. We thank Dr. J. V. Michael for helpful discussions of the adiabatic equation of state method. S.-O.R. and S.M.H. gratefully acknowledge the support of NASA Grant NAG3-1307.

References and Notes

(1) Warnatz, J. In *Combustion Chemistry*; Gardiner, W. C., Jr., Ed.; Springer-Verlag: New York, 1984; Chapter 5.
(2) Baulch, D. L.; Drysdale, D. D.; Horne, D. G.; Lloyd, A. C. *Evaluated Kinetic Data for High Temperature Reactions*; Butterworths: London, 1972; Vol. 1.
(3) Lewis, R. S.; Watson, R. T. *J. Phys. Chem.* **1980**, *84*, 3495.
(4) Howard, M. J.; Smith, I. W. M. *J. Chem. Soc., Faraday Trans. 2*, **1981**, *77*, 997.
(5) Schott, G. L. *Combust. Flame* **1973**, *21*, 357.
(6) Frank, P.; Just, Th. *Ber. Bunsen-Ges. Phys. Chem.* **1985**, *89*, 181.
(7) Schott, G. L. Presented at the Eastern States Section Combustion Institute Meeting, Orlando, FL, Dec 1990.
(8) Gardiner, W. C., Jr.; Walker, B. F.; Wakefield, C. B. In *Shock Waves in Chemistry*; Lifshitz, A., Ed.; Marcel Dekker: New York, 1981; Chapter 7.
(9) McBride, B. J.; Gordon, S.; Reno, M. A. *Coefficients for Calculating Thermodynamic and Transport Properties of Individual Species*; NASA TM-4513; National Aeronautics and Space Administration: Washington, DC, 1993.
(10) Michael, J. V.; Sutherland, J. W. *Int. J. Chem. Kinet.* **1986**, *18*, 409.
(11) Ryu, S.-O. Determination of Rate Coefficients of H + O_2 = OH + O and O + H_2 = OH + H Reactions by Shock Tube − Laser Absorption Spectroscopy. Ph.D. Thesis, University of Toledo, Toledo, 1994.
(12) Frenklach, M.; Wang, H.; Rabinowitz, M. J. *Prog. Energy Combust. Sci.* **1992**, *18*, 47.
(13) Hwang, S. M.; Rabinowitz, M. J.; Gardiner, W. C., Jr. *Chem. Phys. Lett.* **1993**, *205*, 157.
(14) Yuan, T.; Wang, C.; Yu, C. L.; Frenklach, M.; Rabinowitz, M. J. *J. Phys. Chem.* **1991**, *95*, 1258.
(15) Oldenborg, R. C.; Loge, G. W.; Harradine, D. M.; Winn, K. R. *J. Phys. Chem.* **1992**, *96*, 8426.
(16) Michael, J. V. *Prog. Energy Combust. Sci.* **1992**, *18*, 327.
(17) Masten, D. A.; Hanson, R. K.; Bowman, C. T. *J. Phys. Chem.* **1990**, *94*, 7119.
(18) Hindmarsh, A. C. Towards a Systematic Collection of ODE Solvers. Presented at the 10th IMACS World Congress on System Simulation and Scientific Computation, Montreal, Aug 1982.
(19) Gardiner, W. C., Jr. *J. Phys. Chem.* **1977**, *81*, 2367.
(20) Shoemaker, D. P.; Garland, C. W.; Steinfeld, J. I. In *Experiments in Physical Chemistry*; McGraw-Hill: New York, 1974; Chapter 2.
(21) Shin, K. S.; Michael, J. V. *J. Chem. Phys.* **1991**, *95*, 262.
(22) Yang, H.; Gardiner, W. C., Jr.; Shin, K. S.; Fujii, N. *Chem. Phys. Lett.* **1994**, *231*, 449.
(23) Pirraglia, A. N.; Michael, J. V.; Sutherland, J. W.; Klemm, R. B. *J. Phys. Chem.* **1989**, *93*, 282.
(24) Du, H.; Hessler, J. P. *J. Chem. Phys.* **1992**, *96*, 1077.
(25) Frenklach, M. In *Complex Chemical Reaction Systems, Mathematical Modelling and Simulation*; Warnatz, J., Jäger, W., Eds.; Springer-Verlag: Berlin, 1987; p 2.
(26) Michael, J. V.; Fisher, J. R. In *Proceedings of the Seventeenth International Symposium on Shock Waves and Shock Tubes*; Kim, Y. W., Ed.; American Institute of Physics: New York, 1989; p 210.
(27) Yu, C.-L.; Frenklach, M.; Masten, D. A.; Hanson, R. K.; Bowman, C. T. *J. Phys. Chem.* **1994**, *98*, 4770.
(28) Belles, F. E.; Lauver, M. R. In *Proceedings of the Tenth Symposium (International) on Combustion*; The Combustion Institute: Pittsburgh, 1965; p 285.
(29) Schott, G. L.; Kinsey, J. L. *J. Chem. Phys.* **1958**, *29*, 1177.
(30) Fujii, N.; Shin, K. S. *Chem. Phys. Lett.* **1988**, *151*, 461.
(31) Fujii, N.; Sato, T.; Miyama, H.; Shin, K. S.; Gardiner, W. C., Jr. In *Proceedings of the Seventeenth International Symposium on Shock Waves and Shock Tubes*; Kim, Y. W., Ed.; American Institute of Physics: New York, 1989; p 456.
(32) Miller, J. A. *J. Chem. Phys.* **1981**, *74*, 5120.
(33) Miller, J. A. *J. Chem. Phys.* **1986**, *84*, 6170.
(34) Melius, C. F.; Blint, R. J. *Chem. Phys. Lett.* **1979**, *64*, 183.
(35) Varandas, A. J. C.; Brandão, J.; Pastrana, M. R. *J. Chem. Phys.* **1992**, *96*, 5137.
(36) Pastrana, M. R.; Quintales, L. A. M.; Brandão, J.; Varandas, A. J. C. *J. Phys. Chem.* **1990**, *94*, 8073.
(37) "..., their faces were not all the same, yet not unalike, but rather the way sisters ought to be"—Ovid, Metamorphoses 2.13−14.
(38) Sutherland, J. W.; Michael, J. V.; Pirraglia, A. N.; Nesbitt, F. L.; Klemm, R. B. In *Proceedings of the Twenty-First Symposium (International) on Combustion*; The Combustion Institute: Pittsburgh, 1986; p 929.
(39) Dixon-Lewis, G. *Combust. Sci. Technol.* **1983**, *34*, 1.
(40) Albers, E. A.; Hoyermann, K.; Wagner, H. Gg.; Wolfrum, J. In *Proceedings of the Thirteenth Symposium (International) on Combustion*; The Combustion Institute: Pittsburgh, 1971; p 81.

JP9510812